JOURNAL OF GEOPHYSICAL RESEARCH, VOL. 100, NO. B10, PAGES 20,345-20,358, OCTOBER 10, 1995

The March 25, 1990 (M_W=7.0, M_L=6.8), earthquake at the entrance of the Nicoya Gulf, Costa Rica: Its prior activity, foreshocks, aftershocks, and triggered seismicity

Marino Protti,[1] Karen McNally,[2] Javier Pacheco,[3] Victor González,[1] Carlos Montero,[1] Juan Segura,[1] Jorge Brenes,[1] Vilma Barboza,[1] Eduardo Malavassi,[1] Federico Güendel,[1] Gerald Simila,[4] Daniel Rojas,[1] Aaron Velasco,[5] Antonio Mata,[1] and Walter Schillinger[2]

Abstract. On March 25, 1990 a large earthquake (M_W=7.0, M_L=6.8) occurred at the entrance of the Nicoya Gulf, Costa Rica, at 1322:55.6 UTC, producing considerable damage in central Costa Rica and generating much interest about whether or not the Nicoya seismic gap (Nishenko, 1989) had broken. The local country-wide seismographic network recorded 6 years of activity prior to this large earthquake, 16 hours of foreshocks, the mainshock, and its aftershocks. This network is operated jointly by the Costa Rica Volcanological and Seismological Observatory at the National University (OVSICORI-UNA), and the Charles F. Richter Seismological Laboratory at the University of California, Santa Cruz (CFRSL-UCSC). We obtained high resolution locations from this network and located the mainshock at 9°38.5'N, 84°55.6'W (depth is 20.0 km) and the largest foreshock (M_W=6.0, March 25, 1990, at 1316:05.8 UTC) at 9°36.4'N, 84°57.1'W (depth is 22.4 km). We find that the aftershock zone abuts the southeast boundary of the Nicoya seismic gap, suggesting that the seismic gap did not rupture. Since the installation of the local network in April 1984 to March 24, 1990, nearly 1900 earthquakes with magnitudes from 1.7 to 4.8 (318 with magnitude 3.0 or larger) have been located at the entrance of the Nicoya Gulf, one of the most active regions in Costa Rica. The March 25 earthquake occurred at the northwest edge of this region, where a sequence of foreshocks began 16 hours prior to the mainshock. The spatial-temporal distribution of aftershocks and directivity analysis of the mainshock rupture process using teleseismic records both indicate a southeast propagating rupture. The mainshock ruptured an asperity of approximately 600 km^2 of area, with this area expanding to 4000 km^2 after 7 days. We present evidence that suggests that the ruptured asperity is produced by the subduction of a seamount. Inversion of teleseismic broadband and long-period *P* and *SH* waves yields a thrust faulting mechanism with the shallow plane striking 292°, dipping 26°, and with a rake of 88°, in agreement with the subduction of the Cocos plate under the Caribbean plate. Local first motions for the largest foreshock and the mainshock agree with this solution. We also present evidence suggesting that the March 25, 1990, earthquake triggered and reactivated several seismic swarms in central Costa Rica and temporally decreased the activity in the epicentral area of the July 3, 1983 (M_S=6.2), Pérez Zeledón earthquake.

Introduction

Nishenko [1989] calculated that a seismic gap in the Nicoya Peninsula, (Figure 1), Costa Rica, would rupture in a magnitude 7.4 earthquake with 93% probability before the year 2009 (assigned fourth place in Nishenko's list of "top seismic gaps" in the Circum-Pacific). On March 25, 1990, a large earthquake (M_b=6.3, $M_S Z$=7.0 (Preliminary Determination of Epicenters (PDE)), M_W=7.0, M_L=6.8) occurred at the entrance of the Nicoya Gulf, Costa Rica, at 1322:55.6 UTC, near this seismic gap. This earthquake produced considerable damage in central Costa Rica, was felt from southern Nicaragua to western Panama, and generated much interest about whether or not the Nicoya seismic gap had broken (see boundaries in map by *Nishenko* [1989]).

Costa Rica, as part of Central America, is located on the western margin of the Caribbean plate (Figure 1). There, the Cocos plate subducts under the Caribbean plate along the Middle American Trench at a rate between 70 and 94 mm/yr from Guatemala to southern Costa Rica respectively (computed from *De Mets et al.*, [1990]). It is along this plate boundary, at the western coast of Costa Rica, where most of the recent large destructive earthquakes have occurred. Coupling between the Cocos and Caribbean plates changes along strike of the subduction zone in Costa Rica and correlates with the bathymetric characteristics of the subducted oceanic floor: smooth, rough, and rough-smooth ocean floors in northern,

[1]Observatorio Vulcanológico y Sismológico de Costa Rica, Universidad Nacional, Apartado 86-3000, Heredia, Costa Rica.

[2]Charles F. Richter Seismological Laboratory, Institute of Tectonics, University of California, Santa Cruz, California.

[3]Centro de Investigaciones Geofísicas, Universidad de Costa Rica, San Pedro de Montes de Oca, San José, Costa Rica.

[4]Department of Geological Sciences, California State University, Northridge, California.

[5]Science Applications International Corporation, San Diego, California.

Paper number 94JB03099.
0148-0227/95/94JB-03099$05.00

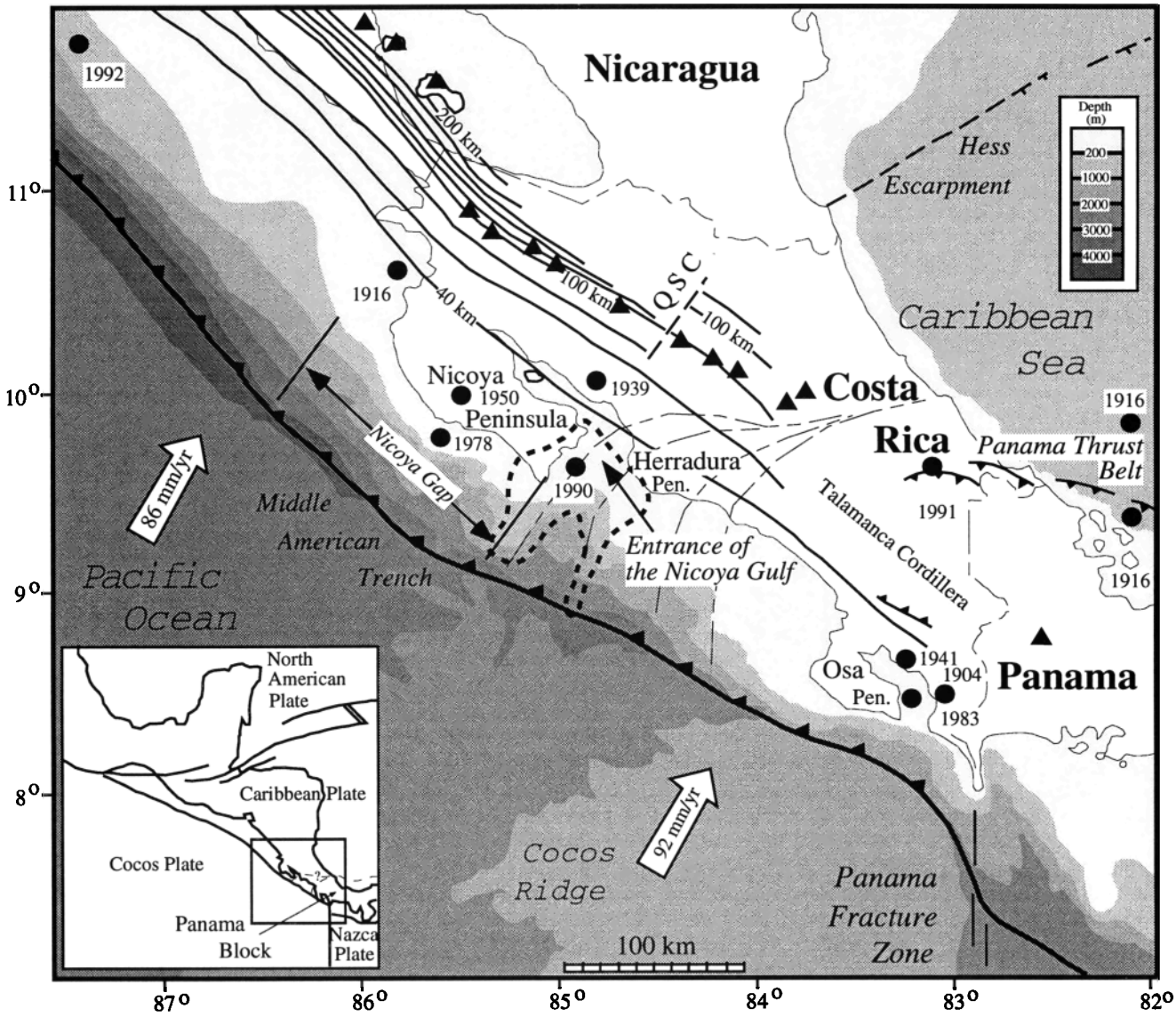

Figure 1. Tectonic setting of southern Central America, geometry of the top of the Wadati-Benioff zone and limits of the Nicoya seismic gap (modified from *Protti et al.* [1994]). Solid triangles are active volcanoes, and solid circles show the location of large ($M_S \geq 7.0$) interplate earthquakes occurred this century. QSC, Quesada Sharp Contortion. Bold dashed line at the entrance of the Nicoya Gulf encloses the aftershock area of the March 25, 1990 (M_W=7.0) earthquake. Thin dashed lines across central Costa Rica schematically represent the shear zone that marks the boundary between the Caribbean plate and the Panama block. Inset map shows the regional tectonic setting of Central America.

central, and southern Costa Rica, respectively [*Protti et al.*, 1994]. *Protti et al.* [1994], suggest that the northern and southern segments of the subduction zone in Costa Rica (under Nicoya and Osa peninsulas, respectively) (Figure 1) have the strongest coupling with the potential to produce events as large as 7.7 in magnitude [*Güendel*, 1986]. In central Costa Rica, the subduction of a rough ocean floor, which consists of isolated sea mountains, appears to reduce the coupling zone to a series of small asperities without potential to generate earthquakes larger than 7.0 [*Protti et al.*, 1994]. We suggest that the March 25, 1990, earthquake ruptured one of these subducting seamounts on the northwest part of Costa Rica's central subduction segment (bounded to the NW and SE by the Nicoya and Osa peninsulas, respectively), right at the contact with the stronger Nicoya segment.

Six years of activity prior to the March 25 event, 16 hours of foreshocks, the mainshock, and its aftershocks were well documented by a local country-wide seismographic network operated jointly by the Costa Rica Volcanological and Seismological Observatory at the National University (OVSICORI UNA), and the Charles F. Richter Seismological Laboratory at the University of California, Santa Cruz (CFRSL UCSC). At the time of the earthquake, this network consisted of 17 telemetered short-period (16 vertical component and one three-component) analog recording stations and one three-component digital strong-motion instrument located at the recording center in Heredia, 100 km from the mainshock location (Table 1) (Figure 2a). In order to better document the aftershock sequence, OVSICORI UNA installed portable seismographs to the east of the epicentral area on the same day

Table 1. OVSICORI UNA's Seismographic Stations

Station	Latitude N	Longitude W	Elevation, m	Operational
CAO	9°42.07'	85°06.20'	263	Nov. 1984 *
CDM	9°33.31'	83°45.95'	3470	April 1984 *
CTCR	8°53.77'	82°45.56'	1620	Jan. 1989 *
DAT	9°41.66'	83°54.93'	2500	Nov. 1989
EPA	9°59.26'	84°35.79'	310	April 1984 *
HDC	10°00.08'	84°06.84'	1157	May 1984 *
HDC2	10°01.42'	84°07.00'	1220	Nov. 1984 *
IDC	8°42.80'	83°52.19'	10	April 1987
IRZ	9°58.47'	83°51.94'	3380	April 1984
IRZ2	9°58.13'	83°53.85'	2950	July 1985 *
JTS	10°17.45'	84°57.15'	340	June 1988 *
JUD	10°09.72'	85°32.82'	844	Nov. 1984 *
OCM	9°53.59'	83°57.65'	1660	June 1989 *
PBC	8°26.62'	83°04.25'	140	March 1985 *
PJS	9°31.70'	84°30.45'	10	March 1990
PLA	9°42.35'	84°40.10'	30	March 1990
POA	10°09.14'	84°13.02'	2093	April 1984
POA2	10°10.63'	84°15.05'	2500	May 1986 *
PT1	11°03.87'	85°25.03'	335	Oct. 1987
PT2	10°54.83'	85°43.21'	10	Oct. 1987
PT3	10°32.74'	85°42.30'	10	Oct. 1987
PT4	9°51.96'	85°28.87'	40	Oct. 1987
PT5	10°57.97'	84°37.70'	90	Nov. 1987
PT6	10°40.42'	85°12.18'	450	Nov. 1987
PT7	10°31.79'	85°15.18'	80	Oct. 1987
PT8	10°17.58'	84°57.19'	350	Oct. 1987
PT9	10°23.53'	84°17.02'	260	Nov. 1987
PT10	10°45.33'	85°00.33'	470	Oct. 1987
PT11	11°02.09'	85°30.31'	290	Nov. 1987
PT12	10°50.42'	85°37.61'	290	Nov. 1987
PT13	11°01.70'	84°43.19'	43	Nov. 1987
PTCR	9°47.37'	84°25.57'	1510	April 1984 *
QPS	9°24.19'	84°07.94'	83	April 1984 *
RIN	10°46.41'	85°21.50'	775	Jan. 1985
RIN2	10°49.11'	85°20.97'	1400	June 1987
RIN3	10°47.45'	85°22.72'	1400	Aug. 1988 *
TIG	9°02.20'	83°17.76'	690	Dec. 1988
VACR	10°28.38'	84°40.65'	360	Sep. 1986 *
VTU	10°01.26'	83°45.50'	3329	March 1990 *

* Stations that recorded the mainshock.

of the earthquake. The temporary network was complemented four days later with four more digital strong-motion instruments sent by the Charles F. Richter Seismological Laboratory of UCSC and the Department of Geology of the California State University at Northridge.

Earthquake Locations

All events were relocated using the program HYPOINVERSE [*Klein*, 1978] and a one-dimensional P wave velocity structure (Figure 2b). In the upper crust this P wave velocity model corresponds to that proposed by *Matumoto et al.*, [1977] for northern Costa Rica, while in the lower crust and upper mantle it corresponds to that obtained by *Zhao et al.* [1992] for northern Honshu, a region tectonically similar to Costa Rica. Locations with this combined model give slightly lower time residuals (RMS) than using only the model by *Matumoto et al.* [1977] or the model by *Zhao et al.* [1992] (Figure 3a). Even though the standard deviations of the RMS for these three models suggest that the difference is not statistically significant, we prefer our combined model because the deep Moho (~43 km) obtained by *Matumoto et al.* [1977] is difficult to reconcile with the thin (20-30 km) crust generally associated with active plate margins. For the S wave velocity structure we used this P wave model and optimized the V_P/V_S ratio by minimizing the overall RMS of 104 events selected from this earthquake sequence. All these selected events are located within the network (gap of < 180) and with 14 or more P and S arrivals. Values of 1.78 and 1.79 (Figure 3a) give the lower overall RMS and standard deviation; we choose 1.78. During this test the mainshock epicenter changed by less than 1 km.

With that value of V_P/V_S ratio, we searched for the best depth to start the iterative earthquake location procedure (parameter ZTR used by HYPOINVERSE), using a sample of over 1000 aftershocks. This parameter has an important effect

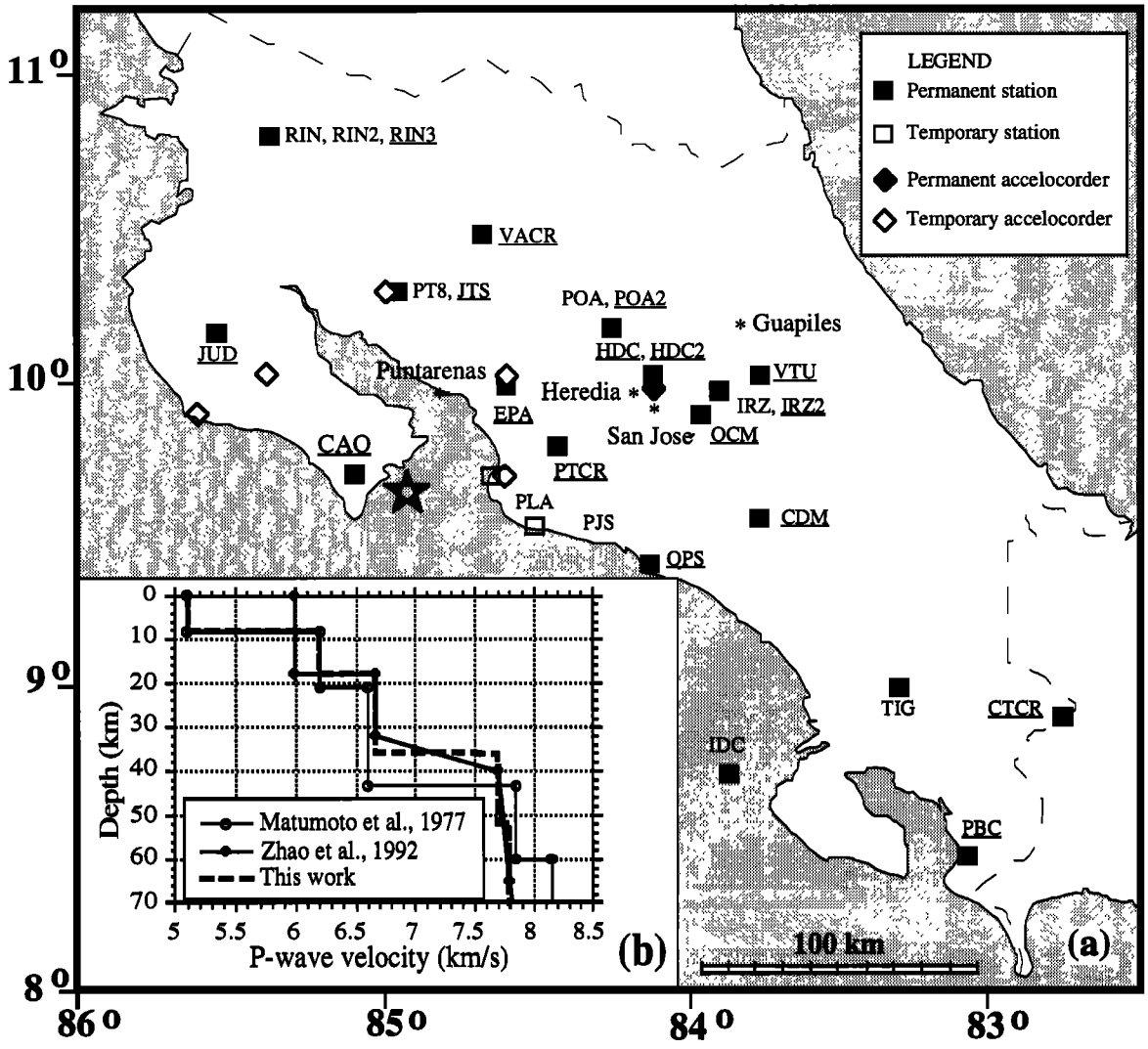

Figure 2. (a) Map showing the configuration of OVSICORI's permanent seismographic network as on March 1990 and the location of temporary stations deployed after the March 25, 1990, earthquake (star). Underlined stations recorded the mainshock. (b) Upper mantle and crustal velocity structures mentioned in the text.

in the final depth especially when it is chosen near the depth of velocity interfaces in the velocity model (in our case 0, 8, 18, and 36 km) (Figure 3b). We found that, ideally, this value should be halfway between velocity boundaries and in the layer where most of the events occur. Since histograms of number of events versus depth for ZTR values of 13 and 27 km (Figures 4a and 4b) show higher concentration of events within the second layer (8-18 km) of our velocity structure, we choose ZTR=13 km to relocate all the events. As an example of the effect of this parameter on earthquake depth, on Figure 3b we also plot the depth computed for the mainshock for each value of ZTR. Events with few observations are not well located by HYPOINVERSE and are placed in or near velocity interfaces (Figure 4c); therefore we excluded them from our database, keeping only events with horizontal and vertical errors lower than 6 and 9 km, respectively. In our relocated database 61% of the events have 12 or more arrival times (including P and S wave arrivals); 70% have an azimuthal gap less than 225°; 71% are at an epicentral distance of less than 40 km to the nearest station; 61% have RMS smaller than 0.25 s; 99% have horizontal errors equal to or smaller than 5 km; and 95% have vertical errors equal to or smaller than 5 km.

Local magnitudes (M_d) are computed by HYPOINVERSE based on the duration of the seismic signal at each station. These duration magnitudes are calculated according to the equation used by OVSICORI UNA in their routine earthquake location procedure (M_d= -1.16 + 2.01 x log T + 0.0035 x D + 0.007 x Z, where T is duration of the event in seconds, D is epicentral distance in kilometers, and Z is focal depth in kilometers) [*Protti et al.*, 1987].

We have divided the following discussions of the seismic activity at the entrance of the Nicoya Gulf into five time stages: (1) prior activity, from April 1, 1984 (beginning of OVSICORI's network catalog), to March 24, 1990; (2) foreshock activity, from March 24, 1990, 2142 UTC to mainshock origin time; (3) mainshock; (4) aftershocks to 100 days after the mainshock, and (5) triggered seismicity.

Prior Activity

The entrance of the Nicoya Gulf (Figure 1) has been identified as one of the most constantly active seismic sources

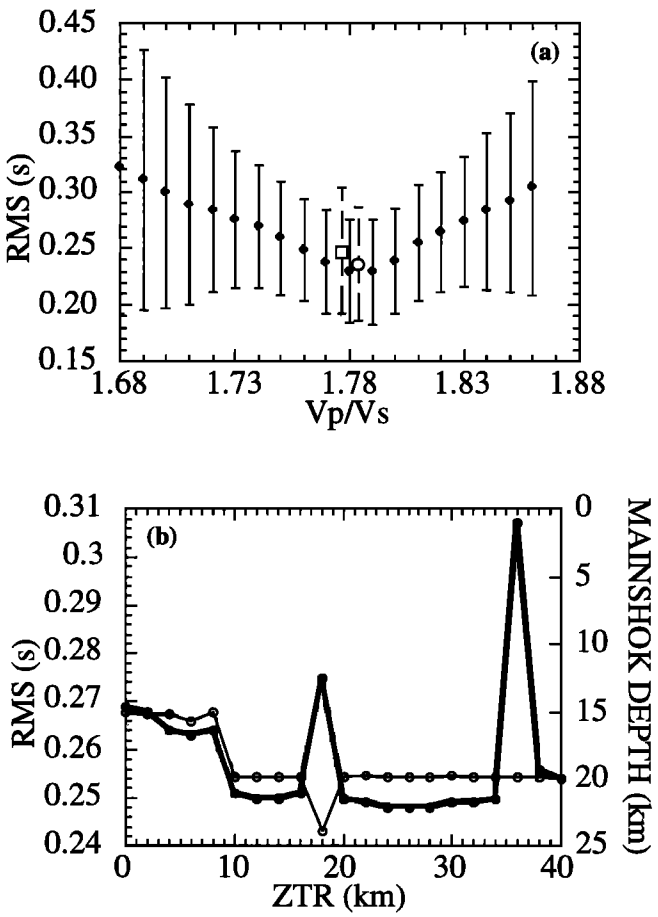

Figure 3. Results of tests for: (a) optimal V_P/V_S ratio, and (b) depth of the first iteration (ZTR) used by HYPOINVERSE, obtained using our proposed velocity structure. Error bars in Figure 3a are two standard deviations; open circle and square are values using the velocity structures by *Matumoto et al.* [1977] and by *Zhao et al.* [1992], respectively. Solid circles in (b) represent values of for a sample of over 1000 aftershocks, while open circles are, for comparison, the depth of the mainshock for the different values of ZTR.

in Costa Rica (OVSICORI UNA's Preliminary Bulletins, 1984-1990 and *Güendel et al.* [1989]). Since the installation of the local network, early in 1984, to March 24, 1990, nearly 1900 earthquakes with duration magnitudes from 1.7 to 4.8 (318 with magnitude 3.0 or larger) have been located in this area. The March 25 earthquake nucleated at the NW border of this region, where a sequence of foreshocks started 16 hours before the mainshock. Most of the activity (the foreshocks, mainshock and early aftershocks) is concentrated in an area of less than 600 km^2 located right at the entrance of the Nicoya Gulf (Figure 5). Other events occurred along a N-S alignment south of this area.

Prior activity shows higher concentration of events landward from the mainshock than aftershock activity. The focal depth of this prior activity shows a bimodal distribution: over 50% of the events have depths between 12 and 17 km and about 35% locate between 20 and 26 km in depth. Local network first-motion focal mechanisms for events with magnitude larger than 4 show dominantly thrust solutions with nodal planes striking parallel to the Middle American Trench (Figure 5). Events near the trench show mainly strike-slip solutions; focal depth for these events is poorly constrained since they are located far from the network and the one-dimensional velocity structure used in the location procedure is less appropriated for events near the trench.

Foreshocks

The March 25, 1990, mainshock was preceded by 16 hours of foreshock activity. At least 12 events occurred in that period that were recorded at station CAO (Figure 2), 20 km west of the mainshock location. The first foreshock occurred on March 24, 2142 UTC with a local magnitude M_d=3.4, 24.8 km deep, and located 7 km ESE from the mainshock (Figure 6). Six more foreshocks were recorded before March 25, 1316:05.8 UTC when the largest foreshock occurred (M_sZ=5.4, M_b=5.8 (PDE), M_w=6.0; 9°36.4'N, 84°57.1'W, depth of 22.4 km), just 6.9 minutes before and only 5 km SW from the mainshock. At least three more foreshocks with magnitudes (coda) larger than 3.5 were recorded on the coda of

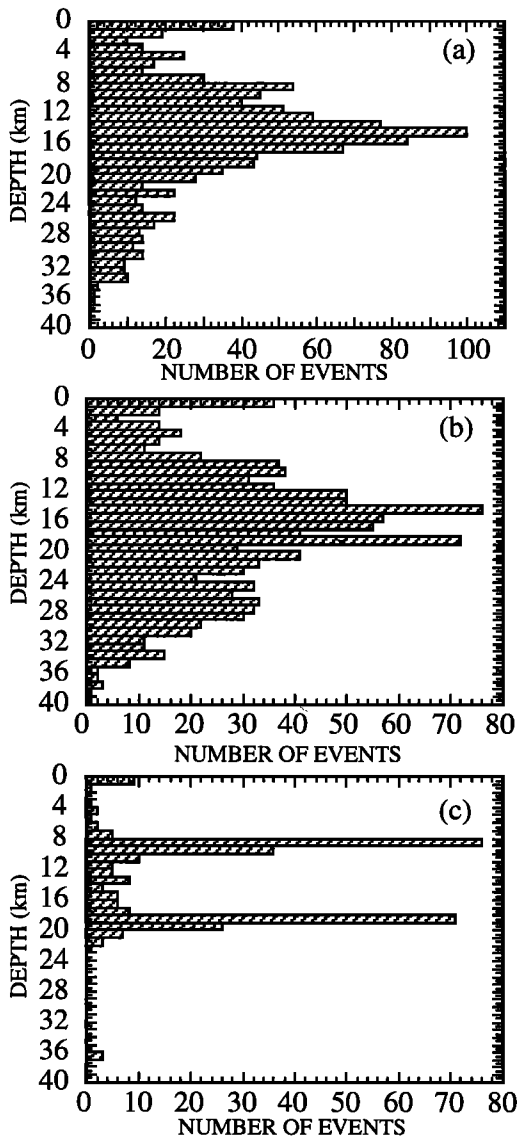

Figure 4. Histograms of number of events versus depth for (a) ZTR=13 km, (b) ZTR=27 km, and (c) for events with location errors in depth (ERZ) greater than 9 km.

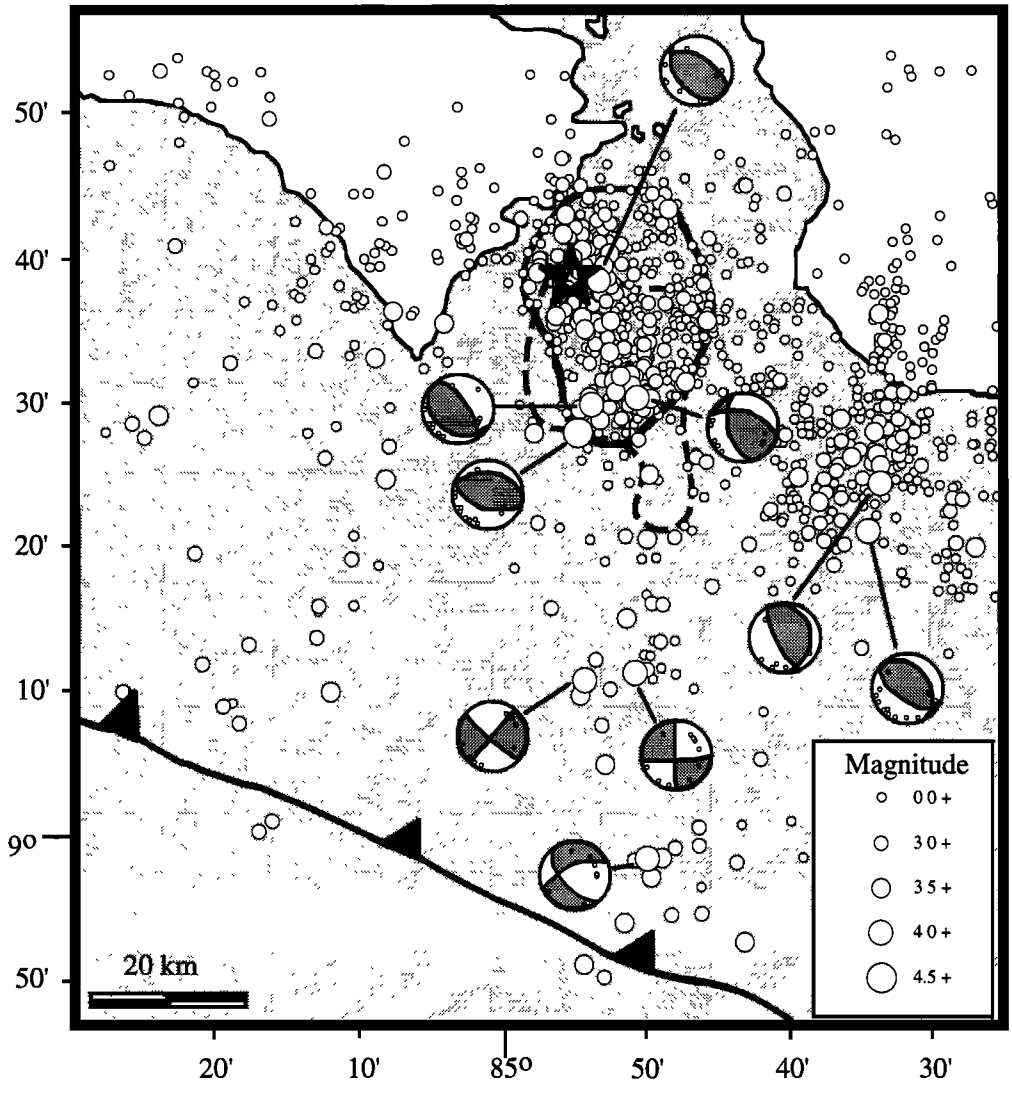

Figure 5. Distribution of seismic activity six years prior to the March 25, 1990 earthquake. The solid line encloses the area with higher activity near the mainshock location (solid star). Also shown are local first-motion focal mechanisms for events with local (coda) magnitude larger than 4.0, and the 1000 minutes (16.7 hours) aftershock area (dashed line).

this largest foreshock. The last foreshock occurred 12 s before the mainshock and had a coda magnitude of about 2.5 (estimated by comparing the maximum amplitude of the recorded offset at each station with the amplitude of the other foreshocks). We were able to locate only six of these foreshocks (Figure 6). These six foreshocks had focal depths between 17 and 28 km. The local network composite first-motion focal mechanism for these six events (Figure 6) gives a thrust solution with the shallow nodal plane subparallel to the Middle American Trench.

We used teleseismic broadband and long-period *P* and *SH* waves (Table 2) to further constrain the source parameters for the largest foreshock. Displacement records are used when broadband stations are available and velocity when only long-period records could be obtained (Table 2). We used all stations available from the tape received from the Incorporated Research Institutions for Seismology (IRIS). No selection was done. The only station not belonging to the IRIS tape and that was explicitly sought is DBN. A least squares procedure develop by *Nábêlek* [1984] is used to obtained the centroid depth, best fitting double-couple solution and the source time history. Our results yield a thrust mechanism with the shallow dipping plane striking 280°, dipping 29°, and a rake of 79° (Figure 7). The centroid depth of 19 km agrees with the hypocenter (or nucleation) depth of 22.4 km. The source time function is composed of a single pulse 8 s long, which yields an apparent stress drop of 0.13 MPa [*Vassiliou and Kanamori* 1982]. Figure 7 also shows the local network first-motion data for this event (triangles). There is a good agreement between the rupture initiation (represented by the first motions) and the average (centroid) mechanism, which suggests a uniform rupture.

Mainshock

The mainshock (M_b=6.3, M_sZ=7.0 (PDE), M_w=7.0, M_L=6.8) of this earthquake sequence at the entrance of the Nicoya Gulf occurred on March 25, 1990, at 1322:55.6 UTC (0722 local time) and was located at 9°38.5'5" latitude north, 84°55.6' longitude west, and at a depth of 20.0 km.

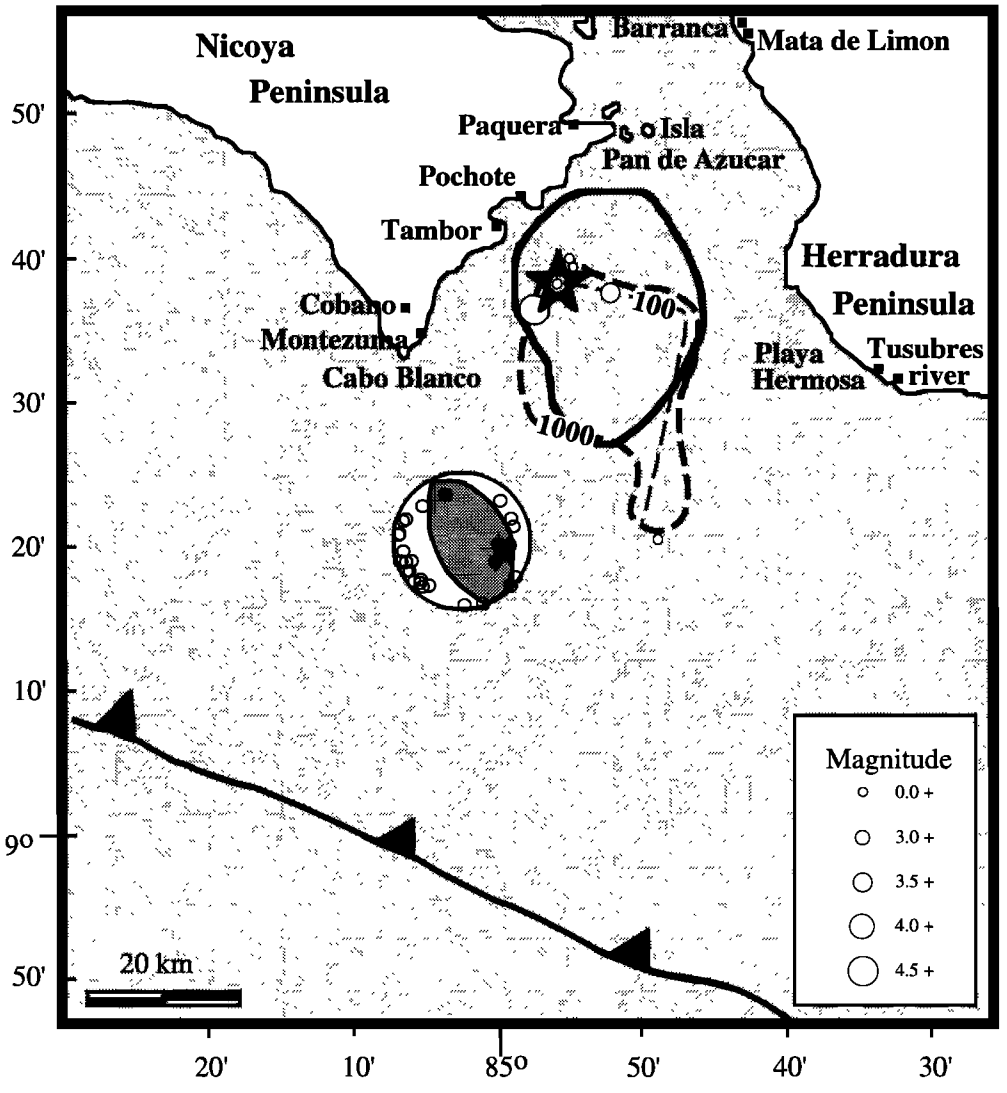

Figure 6. Distribution of the six located foreshocks 16 hours before mainshock (large star) and composite local first-motion focal mechanism for the six foreshocks. For reference, we plot the area of prior activity (solid line), the 100 (thin dashed line), and 1000 (bold dashed line) minutes aftershock zones. Also shown are the location of some of the places mentioned in the text.

We also applied *Nábêlek*'s [1984] procedure on teleseismic waves for the mainshock. The solution for the mainshock has more stations than that for the foreshock because the foreshock is small and therefore the signal to noise ratio in most stations is very low. Using a single source, we obtained a similar mechanism and centroid depth to that obtained for the largest foreshock and a source time function consisting of two large pulses separated in time. The distance and time delay between these two pulses should be sought using the information given by the directivity. Because of the similarities in the solution for the largest foreshock and the mainshock and given their close epicentral location, we decided to use the largest foreshock as an empirical green's function to deconvolve from the mainshock. This deconvolution allows a better resolution on the time history of the mainshock. The criteria to select stations for the deconvolution are basically twofold, the station must be a broadband station, records should exists for both the foreshock and the mainshock, and most importantly, the signal to noise ratio on records for the foreshock should be high. These criteria were satisfied by only the five stations shown in Figure 8. Stations toward the northwest show a longer source time function and a very well defined double pulse, while stations toward the southeast show a much narrower pulse and less defined doublet. The difference in pulse shapes is interpreted here as directivity. Using this information, we applied Nábêlek's procedure with two sources, the results are shown on Figure 9. Both *P* and *SH* waves are well modeled with a double source separated in time by 6 s and 26 km at 124° toward the southeast. The first source is more impulsive, with a 7 s duration and an apparent stress drop of 0.84 MPa, while the second source is longer (12 s) and lower stress drop (0.32 MPa), suggesting a rupture from a stronger toward a weaker zone. Centroid depths for the first and second subevents are 18 and 24 km, respectively. Both subevents occurred on shallow dipping thrusts faults, with slightly different mechanism, whose average (or centroid) is very similar to that of the largest foreshock (strike 292°, dip 26°,

Table 2. Stations Used for the Teleseismic Analysis

Station	Distance	Azimuth	Instrument	Signal
SCP	31.5°	10.3°	broadband	disp (p)
GDH	62.7°	12.0°	long-period	vel (p)
HRV	34.5°	17.5°	broadband	disp (p), disp (sh)
KEV	88.1°	18.8°	long-period	vel (p), vel (sh)
ESK	77.2 °	35.4°	broadband	disp (p), disp (sh)
DBN	82.3 °	38.5°	Galitzi type	vel (p)
TOL	76.7 °	51.3°	broadband	disp (p), disp (sh)
BDF	44.6 °	124.3°	broadband	disp (p), disp (sh)
ZOBO	30.9 °	147.3°	long-period	vel (p)
AFI	89.4 °	255.9°	long-period	vel (p)
KIP	70.8 °	289.3°	broadband	disp (p), disp (sh)
PAS	38.9 °	313.5°	broadband	disp (p), disp (sh)
CMB	42.4 °	317.2°	long-period	vel (p), vel (sh)
COR	47.9 °	323.2°	broadband	disp (p), disp (sh)
ANMO	31.8 °	325.0°	broadband	disp (p), disp (sh)
LON	48.3 °	326.4°	long-period	vel (p), vel (sh)
COL	69.8 °	336.1°	broadband	disp (p), disp (sh)

and rake 88°). Figure 9 shows the average (centroid) mechanism and the first motion data from the local network; again, the agreement suggests the rupture of a single plane.

The local magnitude (M_L=6.8) for the mainshock was obtained from Wood-Anderson seismograms (Figure 10), synthesized, following the method described by *McNally et al.*, [1990], from the records of the acceleroccorder located at OVSICORI UNA's headquarters, 100 km away from the mainshock.

Mainshock Damage

This earthquake reached maximum intensities of VIII (Modified Mercalli) in places up to 60 km away from the earthquake epicenter (Figure 11). No deaths occurred and only 15 people were injured, mostly by broken window glass and masonry and brick falls. The main damage occurred in the towns of Cóbano and Paquera, on the Nicoya Peninsula (20 km NW of the epicenter); in the city of Puntarenas, located on a sand bar 40 km NNE of the epicenter, and at Mata de Limón, an estuary 40 km NE of the epicenter (see Figure 6 for location of these sites). Official reports indicate 34 houses damaged and 8 destroyed; 23 schools damaged and 3 destroyed; 3 buildings severely damaged and 7 slightly damaged.

Rock slides occurred on the road from Tambor to Cóbano and Montezuma and along the sea cliffs from Paquera to Cabo Blanco (southeast border of the Nicoya Peninsula) and along the coastal road and sea cliffs from Barranca to Playa Hermosa (Herradura Peninsula). Rock slides were also reported on an island in the Nicoya Gulf (i.e., Isla Pan de Azúcar). Landslides and rock slides blocked the road linking San José and Guápiles on the Caribbean side.

Liquefaction was documented at the river mouth of the Tusubres river located on the southern tip of Herradura Peninsula (~50 km SE from the mainshock). There were also reports of liquefaction at Pochote and in Mata de Limón.

In Puntarenas, 40 km NNE from the mainshock, most of the damage occurred in the northern section of town, in a mud fill where considerable ground failure and subsidence was

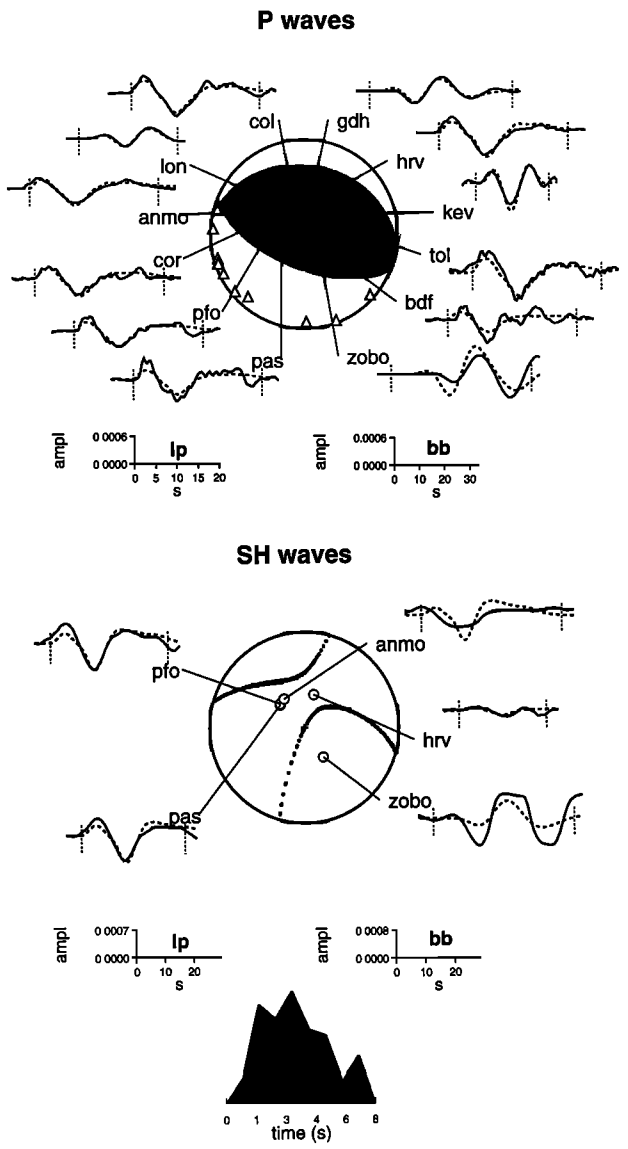

Figure 7. Waveform *P* and *SH* focal mechanism and source time function resulted from our teleseismic inversion for the largest foreshock. Also shown are first motions from local stations.

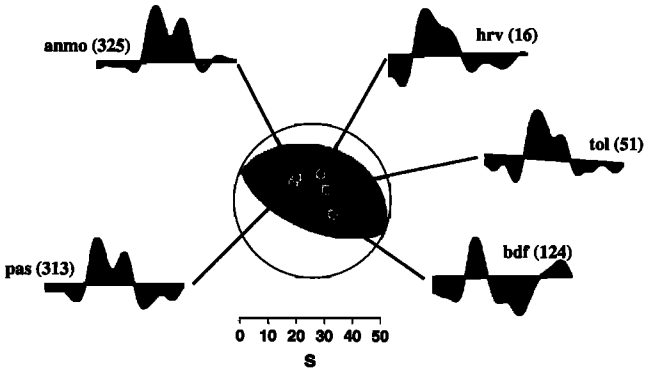

Figure 8. Source time functions for the March 25, 1990, earthquake obtained using the largest foreshock as an empirical Green's function. Numbers in parentheses indicate azimuth in degrees from north.

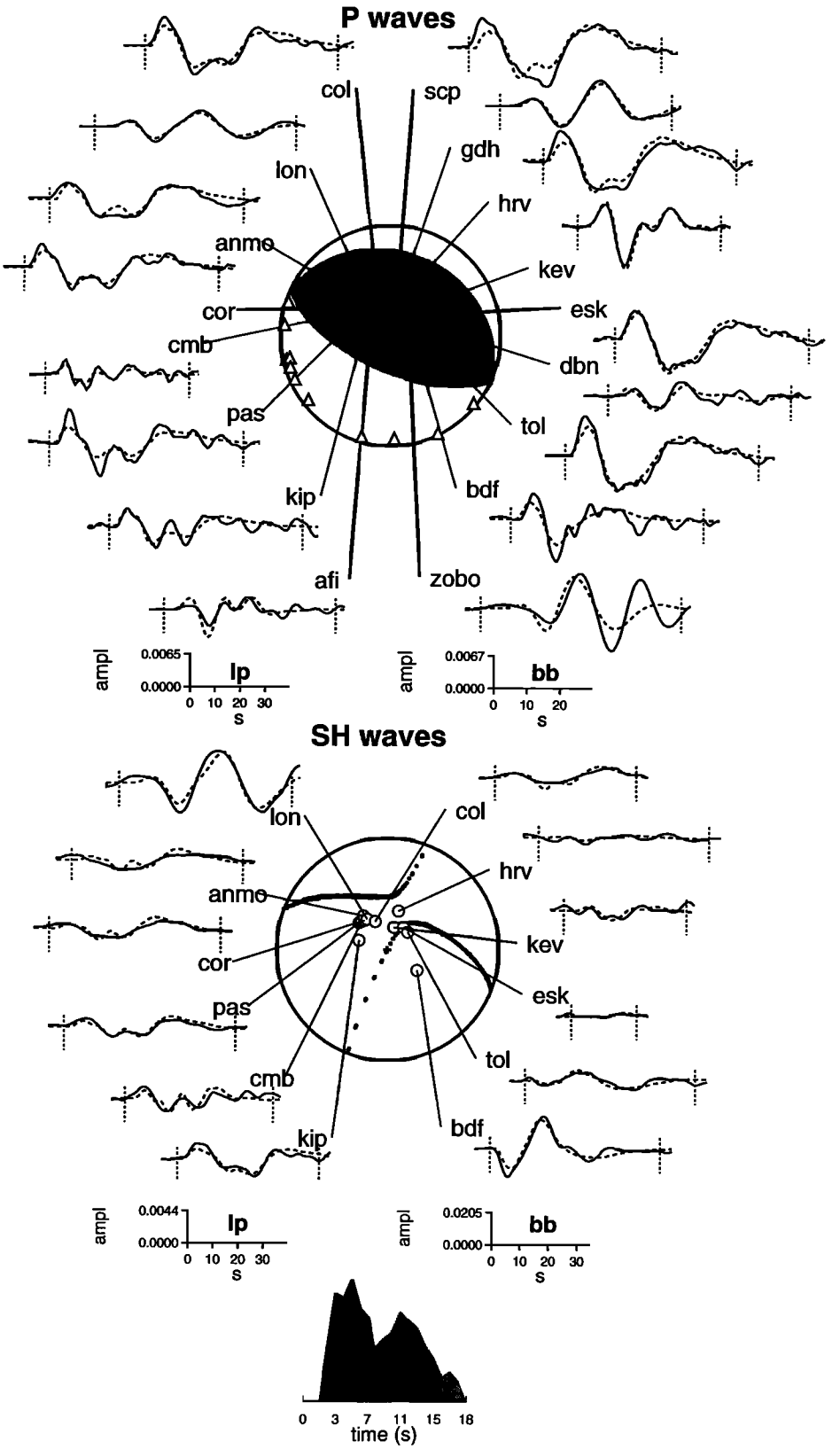

Figure 9. Waveform *P* and *SH* focal mechanism and source time function resulted from our teleseismic inversion for the mainshock. Also shown are first motions from local stations.

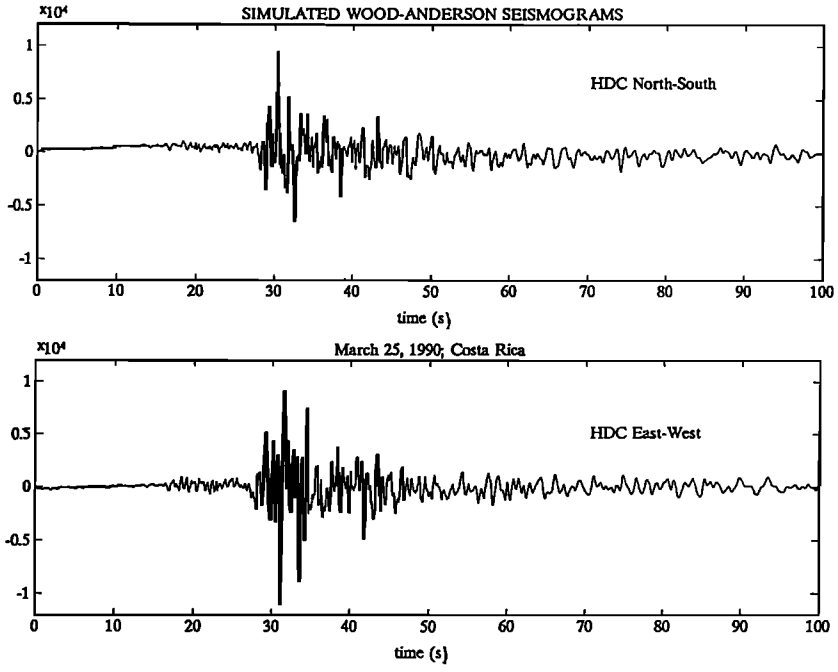

Figure 10. Wood-Anderson seismograms used to compute the local magnitude of the mainshock. This seismograms were simulated from strong-motion records at OVSICORI's recording center (100 km epicentral distance). Vertical scale is in micrometers.

observed. It is important to mention that in this area was also concentrated most of the damage occurred in Puntarenas during the October 5, 1950, Nicoya earthquake (M_S=7.7 [*Pacheco and Sykes*, 1992]), 80 km away. Puntarenas residents who experienced both the 1950 and the 1990 earthquakes, described the ground shaking for the first as much higher than for the recent one.

The 1990 earthquake occurred during low tide, and we recorded, from interviews with local residents, reports of abnormal sea level behavior at two estuaries, in Mata de Limón and at Pochote (Figure 6). There, the sea level reached to half the high tide level in about 5 min after the mainshock and went back to low tide level 5 min later. This behavior was observed for almost three hours after the earthquake.

The intensity pattern of the March 25, 1990, earthquake (solid lines in Figure 11) shows a good correlation with the *S* wave radiation pattern (dotted and dashed lines in Figure 11) computed for the mainshock focal mechanism. This *S* wave radiation pattern was obtained using the program developed and provided by J. Vidale (personal communication, 1990) using the attenuation curves of *Joyner and Boore* [1988].

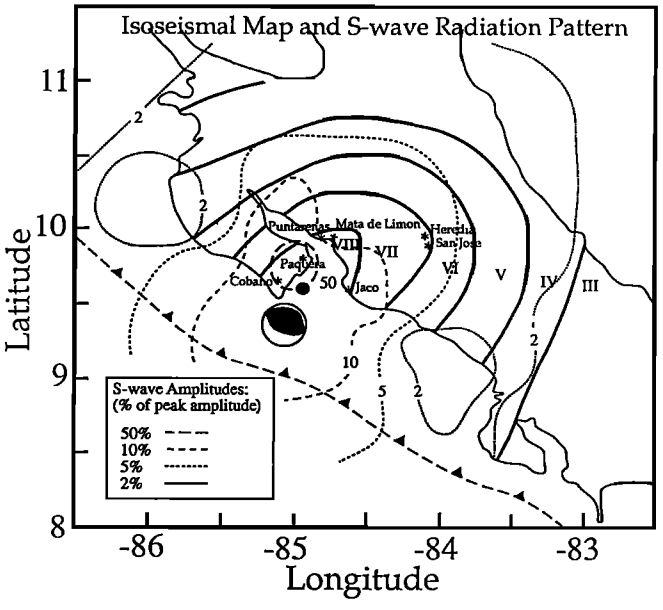

Figure 11. Distribution of maximum modified Mercalli intensities (solid lines) and *S* wave radiation pattern (dotted and dashed lines) for the mainshock. Dashed line with solid tringles indicate the location of the Middle America Trench.

Aftershocks

A count of aftershocks recorded at station CAO shows a decay of activity from over 100 events per hour right after the mainshock to about 30 events per hour, 1 day later. We were able to locate over 1000 aftershocks within 100 days after the mainshock; 50% of them occurred within 10 days after the mainshock.

Early aftershocks (first 1000 min) (16 hours, 40 min) occurred in an area of less than 600 km^2 that increased to nearly 4000 km^2, 10,000 min (6.9 days) after the mainshock (Figure 12a). We note here that the extent of the rupture areas was determined by visual selection, drawing an envelope line enclosing the most conspicuous clusters of activity for each selected time window. The largest aftershock (M_b=5.5, M_sZ=5.3 (PDE), M_d=4.7, 9°23.8N, 84°48.7W, depth of 29.8 km) occurred on March 25 at 2135 UTC (8.3 hours after and 30 km southeast from the mainshock). Most aftershocks occurred in this direction, some extending up to 100 km in the form of isolated clusters. Within 100 days almost the entire Costa Rica's central subduction segment, bounded by the Nicoya and Osa peninsulas, had events with magnitudes 2.5 or larger. The

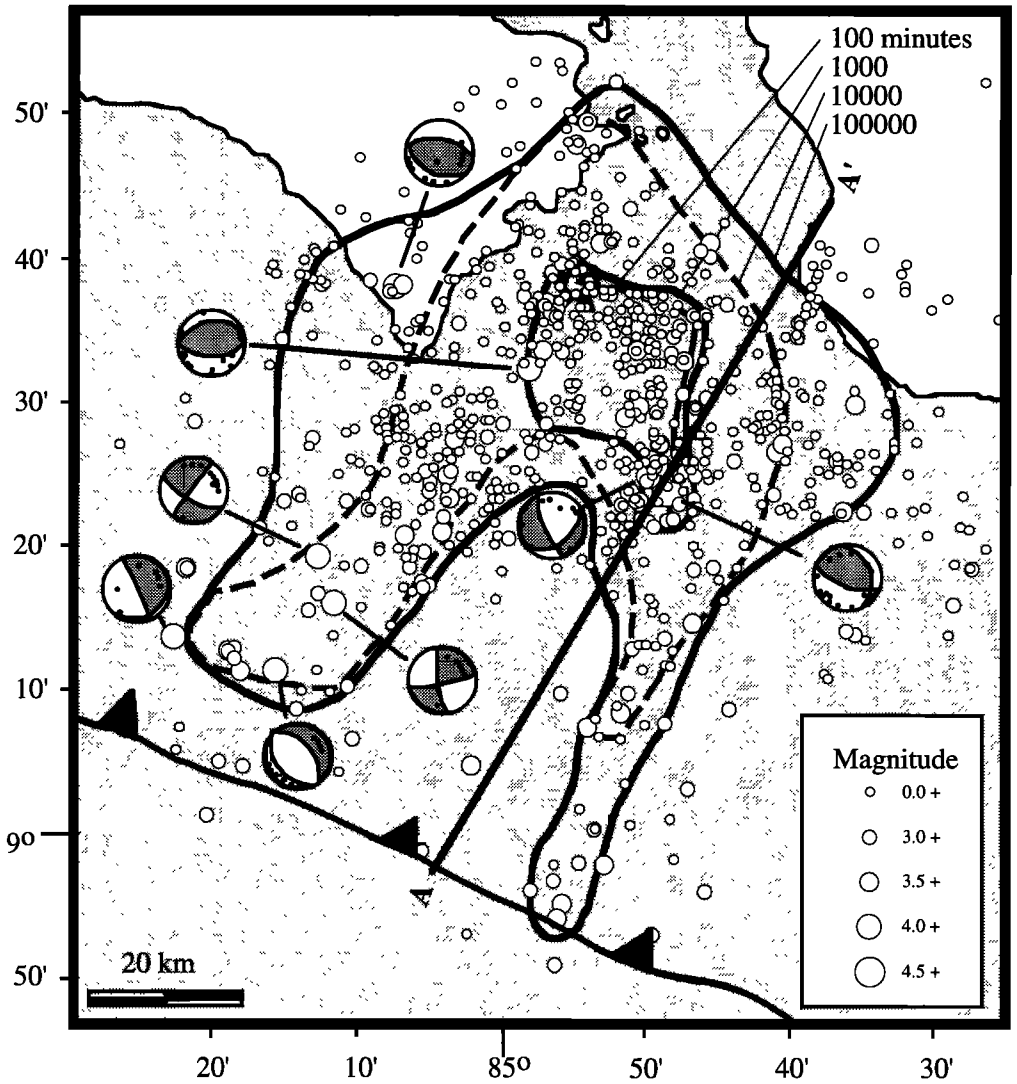

Figure 12a. Distribution of events 100 days after the mainshock and local first-motion focal mechanisms for aftershocks with local (coda) magnitude larger than 4.0. Solid and dashed lines represent (outwards) the 100, 1000, 10,000 and 100,000 min aftershock areas.

normally large background activity of the central segment at this magnitude threshold makes difficult, after 3 months, to differentiate aftershocks from background activity. Very few aftershocks occurred under the Nicoya peninsula, NW from the mainshock.

A cluster of aftershocks occurred trenchward from the rupture zone 2 days after the mainshock. The location, depth and composite focal mechanism (Figures 12a and 12b) suggest that these events are not part of the underthrust rupture but are extensional intraplate events produced by the down dip pull induced by slippage in the mainshock and immediate aftershocks [*Christensen and Ruff*, 1988; *Liu and McNally*, 1993].

Triggered Seismicity

As part of after-mainshock activity, we noted an increment of shallow (depth < 20 km) upper plate seismic activity in the form of several swarms in central Costa Rica, 60 to 120 km ENE from the mainshock (subareas 1, 2, and 3 in Figure 13). This increment started 8 to 36 hours after the mainshock (Figure 13d), and their proximity in time and space suggest that they were the result of important change in the static stress field induced by the mainshock slip. This change in the static stress field could also be responsible for the decrease in activity in another swarm 140 km ESE from the mainshock (subarea 5 in Figure 13). This last seismic swarm area has been active since the occurrence of the July 3, 1983 (M_S=6.2), Pérez Zeledón earthquake [*Güendel et al.*, 1989]. Subarea 4 in Figure 13 did not show significant changes in seismicity.

Discussion

The location of the 1990 earthquake, its foreshocks, and its aftershocks clearly suggest that this event did not break the Nicoya gap. Thus the seismic potential of 93% for a large earthquake in Nicoya, Costa Rica, calculated by *Nishenko* [1989], if correct, still exists. Furthermore, the facts that the mainshock and largest foreshock occurred right at the contact with the Nicoya gap, the unilaterally rupture propagation to

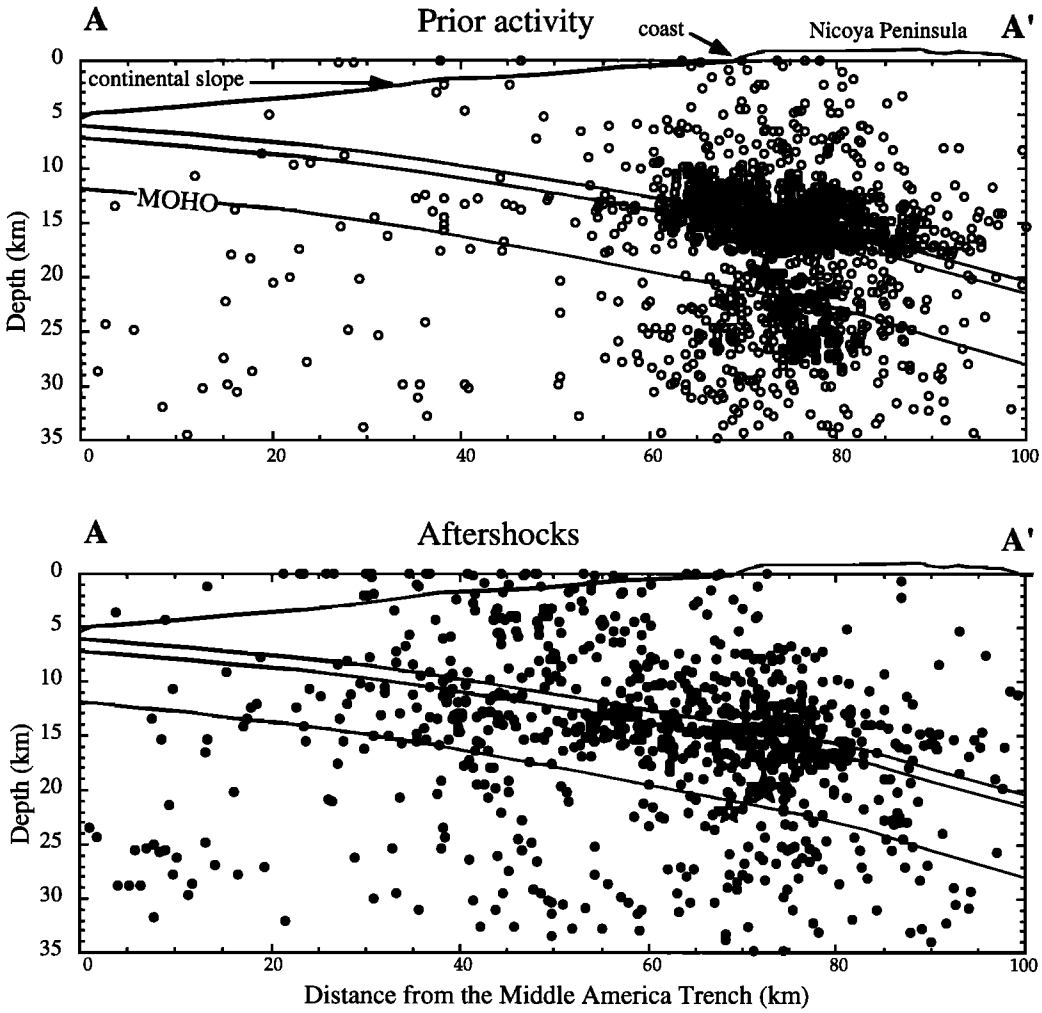

Figure 12b. Cross sections of seismicity (top) prior to and (bottom) after the March 25, 1990, earthquake. Open and solid stars indicate the location of the largest foreshock and mainshock respectively. The geometry of the subduction zone was obtained by *Fluh et al.* [1992] from a seismic refraction survey near and parallel to the profile line. Thin layer at the top of the slab represents the upper oceanic crust.

the SE, and the occurrence of only a few aftershocks under the SE part of the Nicoya peninsula suggest a much stronger coupling for the Nicoya segment. The boundary between the Nicoya and central Costa Rica subduction segments coincides with, or corresponds to, the downdip extension of the "rough-smooth boundary" of *Hey* [1977] and with the updip extension of the Quesada sharp contortion (QSC) [*Protti et al.*, 1994]. We observed the same rupture propagation pattern after the September 2, 1992, Nicaragua (M_S=7.2 (PDE)) earthquake whose aftershock area shows an abrupt termination just NW of the Nicoya peninsula. We used these sudden terminations of the aftershock areas of these two large earthquakes (Costa Rica 1990 and Nicaragua 1992) to mark the SE and NW limits of the Nicoya gap (Figure 1).

Teleseismic locations for subduction earthquakes along the Pacific coast of Costa Rica tend to be shifted landward 40 to 70 km NE [*Güendel*, 1986]. This, together with the magnitude and relative distribution of aftershocks (International Seismological Service (ISS) bulletin, 1939) make us believe that the December 21, 1939, M_S=7.1 [*Pacheco and Sykes*, 1992], earthquake (Figure 1) ruptured the same region as the 1990 earthquake. This gives a crude recurrence time of 50 years; going 50 years back from 1939 take us to the 1880s when indeed an earthquake with similar intensity patterns as the 1990 event occurred on March 3, 1882 [*González-Víquez*, 1910]. That event produced damage in Puntarenas and in central Costa Rica, and most of its aftershocks were only reported felt in Puntarenas [*González-Víquez*, 1910]. Earthquake catalogs are not complete enough to extract other events from this region leaving a still crude recurrence time for the entrance of the Nicoya gulf of 54 ± 4 years.

The absence of events with magnitude larger than 7.0 in this central part of the subduction zone in Costa Rica, as shown by *Protti et al.* [1994], implies a low interplate coupling along small asperities as a product of the subduction of rough seafloor. The characteristics of this rough ocean floor were discussed by *Hey* [1977], by *Londsdale and Klitgord* [1978], and, more recently, by *Von Huene et al.* [1994], who imaged in great detail both the seamounts to be subducted as well as those already under the outer arc. The 1990 earthquake ruptured one of these asperities. Both prior activity and aftershocks define a V-shaped feature pointing in the direction of the subduction. This feature mimics a gorge in the continental slope (Figure 1) left by tectonic erosion caused by

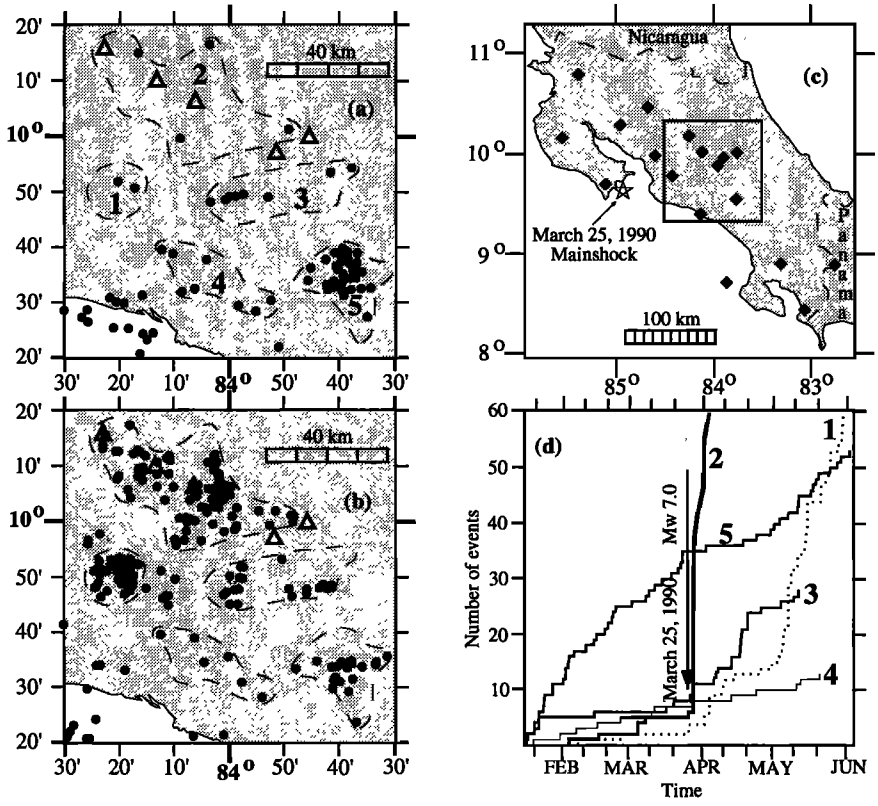

Figure 13. Shallow (depth < 20 km) upper plate seismicity (solid circles) in central Costa Rica 100,000 minutes (~70 days) (a) before and (b) after the March 25, 1990 earthquake. (c) Location of regions in Figure 13a and 13b together with the network distribution. (d) Temporal distribution of activity in sub-areas 1 through 5. Open triangles and solid diamonds indicate the location of active volcanoes and seismographic stations, respectively.

the subduction of a sea mountain chain [*Von Huene et al.*, 1994], suggesting an important role of subducted sea mountains in the interplate coupling. The fact that we can resolve details of the rupture area indicates also the importance of these local studies of aftershocks for the understanding of subduction processes, details that otherwise will not be recorded by global or regional networks.

Prior activity (6 years) shows that the asperity that ruptured during the 1990 earthquake produced by the subduction of a seamount did not show the characteristic doughnut pattern observed before the rupture of larger asperities [*Mogi*, 1981] but instead showed a large concentration of events inside and around the asperity. This might indicate a profound difference between this type of asperities and those existing where smooth ocean floor subducts (i.e., under the Nicoya peninsula). The three-dimensional characteristics of the plate interface in regions where sea mountains are subducted may induce not only intense deformation of the upper plate at the outer arc but also internal breakdown of the sea mountain itself, providing for a larger background seismicity with a large range in depth prior to rupturing with large earthquakes. Figure 12b shows this volumetric distribution of activity, prior and after the main rupture, and its relationship with the plate interface, according to the model suggested by *Fluh et al.* [1992]. The mainshock nucleated in a relatively quiet region between two clusters of prior activity, just below the plate interface; the largest foreshock seems to be part of the deeper cluster. Aftershocks locate mainly on and above the plate interface. This pattern of seismicity may suggest that brittle deformation of the sea mountain occur mainly during accumulation of strain at the locked plate interface prior to main rupture. We note here that even though the structure model by *Fluh et al.* [1992] is preliminary, the location of the interface is not expected to change by more than a couple of kilometers.

Even though the depths of events near the trench are not well resolved by the local network, these events have a relatively deep sources and their first-motion focal mechanisms (Figures 5 and 12) suggest an intraplate outer rise source. The remarkable N-S alignment of prior activity along 84°50'W and the occurrence of strike-slip mechanisms (Figure 5) also suggest motion along a preexisting transform fault on the subducting plate, probably the fault offsetting the Galapagos and Ecuador rifts (see Figure 9 of *Protti et al.* [1994]).

The good correlation between the intensity pattern and the theoretical *S* wave radiation pattern (Figure 11) is of potential importance for studies to predict future ground shaking and damage induced by large subduction earthquakes along the Pacific coast of Costa Rica.

Conclusions

The March 25, 1990, earthquake that occurred at the entrance of the Nicoya Gulf, was the best documented large earthquake in Costa Rica to date, and was one of the best

locally recorded subduction earthquakes around the circum-Pacific region. Teleseismic waveform modeling of this earthquake reveals a thrust faulting mechanism consistent with the subduction of the Cocos plate under the Caribbean plate. Rupture propagated SE from the location of mainshock initiation. The analyses of the data recorded locally are in agreement with those from waveform information recorded teleseismically (i.e., magnitude, fault plane solutions, and rupture propagation).

The NW extension of the rupture zone, where the foreshocks and the mainshock occurred, marks the SE boundary of the Nicoya gap and is coincident with the SW extension of a sharp contortion (the Quesada sharp contortion) [*Protti et al.*, 1994] affecting the subducted slab under central Costa Rica (Figure 1). Only a small corrosion of the interplate coupling zone occurred NW of that boundary (under Nicoya peninsula), indicating that this earthquake did not break the Nicoya gap and that stronger plate coupling exists in that region.

The 1990 earthquake at the entrance of the Nicoya Gulf apparently ruptured a small asperity created by the subduction of a seamount. We have shown the importance of local network studies of aftershocks for both (1) resolving details of the rupture area that otherwise would not be recorded by global or regional networks, and (2) for the understanding of subduction processes.

The occurrence of the March 25, 1990, earthquake apparently triggered swarm activity in some areas and suppressed activity in another swarm, within the overriding upper plate.

Acknowledgements. Ileana Arauz, Luis Arrollo, Jorge Barquero, Oscar Barrantes, Juan Bravo, Franklin De Ovaldía, Eliecer Duarte, Eric Fernández, Ligia Hernando, Tomas Marino, Ora Patterson, Freddy Saborío, Wilgem Vahrson and the Costa Rica Emergency Commission contributed in the collection of damage reports. John Vidale provided a copy of his code for the *S* wave radiation pattern. Kirk McIntosh corrected an error we had in our program to compute plate velocities. Jaime Urrutia-Fucugauchi, Luciana Astiz, Susan Schwartz, and an anonymous referee made valuable suggestions to improve the manuscript. This research was partially funded by NSF grant EART-9115667 to K. McNally. Facilities support and field instrumentation were provided by the W. M. Keck Foundation. Contribution No. 168 of the Observatorio Vulcanológico y Sismológico de Costa Rica and contribution No. 227 of the Institute of Tectonics.

References

Christensen, D. H., and L. J. Ruff, Seismic coupling and outer rise earthquakes, *J. Geophys. Res., 93*, 13,421-13,444, 1988.

De Mets, C., R.G. Gordon, D.F. Argus, and S. Stein, Current plate motions, *Geophys. J. Int., 101*, 425-478, 1990.

Fluh, E.R., S. Ye, A. Stavenhagen, G. Leandro, and J. Bialas, Pacomar, Sonne 76, Compilation of seismic data: GEOMAR-data-report, Res. Cent. for Mar. Geosci., Christian-Albrechts Univ., Kiel, Germany, 1992.

González-Víquez, C., *Temblores, Terremotos, Inundaciones y Erupciones Volcánicas en Costa Rica, 1608-1910*, 200 pp., Tipografía de Avelino Alsina, San José, Costa Rica, 1910.

Güendel, F., Seismotectonics of Costa Rica: An analytical view of the southern terminus of the Middle America Trench, doctoral dissertation, Univ. of Calif., Santa Cruz, 1986.

Güendel, F., et al., First results from a new seismographic network in Costa Rica, Central America, *Bull. Seismol. Soc. Am., 79*, 205-210, 1989.

Hey, R. N., Tectonic evolution of the Cocos-Nazca spreading center, *Geol. Soc. Am. Bull., 88*, 1404-1420, 1977.

Joyner, W. B., and D. M. Boore, Measurement, characterization, and prediction of strong ground motion, paper presented at Conference on Earthquake Engineering and Soil Dynamics II, Geotech. Eng. Div. Am. Soc. of Civ. Eng., Park City, Utah, June 27-30, 1988.

Klein, F. W., Hypocenter location program HYPOINVERSE, *U.S. Geol. Surv. Open File Rep.78-694*, 113 pp., 1978.

Liu, X., and K. McNally, Quantitative estimates of interplate coupling inferred from outer rise earthquakes, *Pure Appl. Geophys., 140*, 211-255, 1993.

Londsdale, P. F., and K. D. Klitgord, Structure and tectonic history of the eastern Panama basin, *Geol. Soc. Am. Bull., 89*, 981-999, 1978.

Matumoto, T., M. Othake, G. Latham, and J. Umaña, Crustal structure of southern Central America, *Bull. Seismol. Soc. Am., 67*, 121-134, 1977.

McNally, K.C., J. Yellin, M. Protti-Quesada, G. Simila, E. Malavassi, W. Schillinger, R. Terdiman, and Z. Zhang, The local magnitude of the 18 October 1989 Santa Cruz Mountains earthquake is M_L=6.9, *Geophys. Res. Lett., 17*, 1781-1784, 1990.

Mogi, K., Seismicity in western Japan and long-term earthquake forecasting, in *Earthquake Prediction: An International Review, Maurice Ewing Ser.*, vol. 4, edited by D.W. Simpson and P.G. Richards, pp. 43-51, AGU, Washington, D.C., 1981.

Nábêlek, J., Determination of earthquake source parameters from inversion of body waves, Ph.D. thesis, Mass. Inst. of Technol., Cambridge, 1984.

Nishenko, S. P., Circumpacific seismic potential 1989-1999, *U.S. Geol. Surv. Open File Rep. 89-86*, 1989.

Pacheco, J. F., and L. R. Sykes, Seismic moment catalog of large shallow earthquakes, 1900 to 1989, *Bull. Seismol. Soc. Am., 82*, 1306-1349, 1992.

Protti Quesada, M., V. González, and F. Güendel, Earthquake catalog 1986, 151 p., Obs. Vulcanol. y Sismol. de Costa Rica, Heredia Univ. Naci., 1987.

Protti, M., K. McNally, and F. Güendel, Correlation between the age of the subducting Cocos Plate and the geometry of the Wadati-Benioff zone under Nicaragua and Costa Rica, in *Geologic and Tectonic Development of the Caribbean Plate Boundary in Southern Central America*, edited by P. Mann, Geological Society of America, Boulder, Colo., in press, 1994.

Vassiliou, M. S. and H. Kanamori, The energy release in earthquakes, *Bull. Seismol. Soc. Am., 72*, 371-378, 1982.

Von Huene, et al., Morphotectonic features of the Costa Rican Pacific margin surveyed during the Sonne 76 cruise, iin *Geologic and Tectonic Development of the Caribbean Plate Boundary in Southern Central America*, edited by P. Mann, Geological Society of America, Boulder, Colo., in press, 1994.

Zhao, D., A. Hasegawa, and S. Horiuchi, Tomographic imaging of P and S wave velocity structure beneath northeastern Japan, *J. Geophys. Res., 97*, 19,909-19,928, 1992..

V. Barboza, J. Brenes, V. González, F. Güendel, A. Mata, C. Montero, and M. Protti-Quesada, Observatorio Vulcanológico y Sismológico de Costa Rica, Universidad Nacional, Apartado 86-3000, Heredia, Costa Rica.(e-mail: jprotti@irazu.una.ac.cr; protti@rupture.ucsc.edu)

K. McNally and W. Schillinger, Charles F. Richter Seismological Laboratory, Institute of Tectonics, University of California, Santa Cruz, California 95064.

J. Pacheco, Centro de Investigaciones Geofísicas, Universidad de Costa Rica, San Pedro de Montes de Oca, San José, Costa Rica.

G. Simila, Department of Geological Sciences, California State University, Northridge, California 91330.

A. Velasco, Science Applications International Corporation, 10260 Campus Point Dr., San Diego, CA 92024

(Received December 27, 1993; revised November 21, 1994; accepted November 29, 1994.)